FILE COPY
NO 3

NACA RM L51E09

NACA

RESEARCH MEMORANDUM

WING-FLOW STUDY OF PRESSURE-DRAG REDUCTION AT TRANSONIC SPEED BY PROJECTING A JET OF AIR FROM THE NOSE OF A PROLATE SPHEROID OF FINENESS RATIO 6

By Mitchell Lopatoff

Langley Aeronautical Laboratory
Langley Field, Va.

THIS DOCUMENT ON LOAN FROM THE FILES OF
NATIONAL ADVISORY COMMITTEE FOR AERONAUTICS
LANGLEY AERONAUTICAL LABORATORY
LANGLEY FIELD, HAMPTON, VIRGINIA
RETURN TO THE ABOVE ADDRESS.
REQUESTS FOR PUBLICATIONS SHOULD BE ADDRESSED AS FOLLOWS:
NATIONAL ADVISORY COMMITTEE FOR AERONAUTICS
1512 H STREET, N. W.
WASHINGTON 25, D. C.

NATIONAL ADVISORY COMMITTEE
FOR AERONAUTICS

WASHINGTON
October 26, 1951

NATIONAL ADVISORY COMMITTEE FOR AERONAUTICS

RESEARCH MEMORANDUM

WING-FLOW STUDY OF PRESSURE-DRAG REDUCTION AT TRANSONIC SPEED BY PROJECTING A JET OF AIR FROM THE NOSE OF A PROLATE SPHEROID OF FINENESS RATIO 6

By Mitchell Lopatoff

SUMMARY

A study was made at transonic speeds by the NACA wing-flow method of the pressure-drag reduction obtained by projecting a high-energy jet of air from the nose of a prolate spheroid. Supplementary information was obtained by taking shadowgraphs of the model mounted in a small supersonic tunnel at a constant Mach number of 1.5.

The high-velocity jet was observed to alter the pressure distribution over the body in such a way that the pressure drag of the body was reduced; thus, in a restricted sense, the nose jet produced a thrust on the body. Under the conditions investigated, the thrust produced by the nose jet was never so large as that which would be expected from a conventional rearward jet. For example, under the best conditions tested (Mach number of 1.07) the reduction in body pressure drag caused by the nose jet more than compensated for the negative thrust of the jet itself. However, the magnitude of the net reduction in drag (change in body pressure drag with jet on and jet off minus the adverse thrust of the jet) was only about one-half of the thrust which would be produced by the same jet exhausting rearward. The appearance of such an unexpectedly large effect in the first trial indicates the phenomenon to be worth further study.

INTRODUCTION

The National Advisory Committee for Aeronautics is conducting a general investigation to determine the drag of bodies at transonic speeds. A method for reducing the drag, described in reference 1,

consists of increasing the forebody fineness ratio. In a review of the literature, however, it was noted in reference 2 that body drag may also be reduced by release of energy in the form of a transverse flame from the nose of the body. In a more recent study (reference 3) the combustion of fuel ejected from the nose of the body is considered as a means of propulsion. The possibility has also been suggested that energy in the form of a high-velocity jet of air issuing from the body nose might also reduce drag. The exploratory investigation reported herein was conducted to determine the possible usefulness and effectiveness of this latter method. The study was conducted at transonic speeds using the wing-flow technique on a prolate spheroid of fineness ratio 6.

SYMBOLS

a	speed of sound, feet per second
A	area, square feet
C_D	pressure-drag coefficient
C_T	thrust coefficient (positive when acting in the direction of flight)
$\frac{dp}{dt}$	rate of change of pressure in accumulator, pounds per square foot per second
L	total length of body
M	Mach number
p	local static pressure
p_0	stream static pressure
P	pressure coefficient $\left(\frac{p - p_0}{q} = \frac{\Delta p}{q}\right)$
q	stream dynamic pressure
r	radius at any point on the body
R	maximum radius of body

TRF thrust recovery factor $\left(\frac{\left(C_{D_j} - C_D\right) - C_T}{C_T}\right)$

V volume of accumulator, cubic feet

x distance from the nose

γ ratio of specific heat at constant pressure to specific heat at constant volume

Subscripts:

ex exit

1 initial condition in accumulator

j with jet on

max maximum

m model

s static

APPARATUS AND METHOD

The prolate spheroid model used in this investigation is shown in figures 1 and 2 as a sketch and photograph, respectively. The dimensions and orifice locations of this body (with a fineness ratio of 6 and an elliptical profile) are shown in figure 1. The upper and lower meridians each carried 13 static-pressure orifices spaced along the body. The upper- and lower-surface orifice at a given position x/L were tied into a single pressure line at the center of the body. By this means, the average pressure for upper and lower surface was measured and tends to compensate for any small misalinement of the model. The average pressure was assumed to represent the pressure at zero angle of attack. A single orifice of 0.032 inch in diameter was placed in the nose of the model to be used as the exit for the high-energy jet involved in this experiment. The body-sting combination was mounted 6 inches above the airplane wing as shown in figure 3 and was alined laterally with the local flow.

The model Mach number was determined by measurements from the reference static-pressure tube located 8 inches to the left of the model

position shown in figure 3. The static-pressure tube was calibrated by placing a survey pressure tube in the model position and recording simultaneously both the survey and reference pressures during a test-procedure run. The Mach number at the model position was obtained from the average static pressures measured along the axis of the model and is shown in figure 4 as a function of the Mach number at the reference static tube. The static orifice on the reference static tube was placed well in front of the nose of the model to eliminate any interference from the model in recording Mach number. There was no indication that the reference static tube interfered with recording model pressures.

Continuous records of all model pressures and supplementary information such as airplane impact and static pressures were recorded during a dive from an altitude of 28,000 feet and a Mach number of approximately 0.50 to 15,000 feet and a Mach number of about 0.71 which gave corresponding model Mach numbers of 0.70 to 1.10, respectively. The Reynolds number based on a body length of 6 inches varied from 0.80×10^6 to 1.10×10^6. A number of 10-second records at a constant Mach number were also obtained to supplement data recorded in the dive.

Additional equipment installed in the ammunition compartment of the aircraft consisted of an accumulator with a capacity of 69 cubic inches, solenoid valve, and a high-pressure recorder. During the short 10-second runs, a switch operated by the pilot was turned on for approximately 2 seconds, which released the compressed air retained in the accumulator through the nose jet. The accumulator pressure varied from 308 pounds per square inch to 163 pounds per square inch during the test.

A small supersonic tunnel (reference 4) as shown in figure 5 was used to take shadowgraphs of the wing-flow model set up in the tunnel at a Mach number of 1.5.

RESULTS AND DISCUSSION

Pressure distributions along the body axis.- The basic data are presented as the variation of pressure coefficient $\Delta p/q$ with each orifice position x/L for several different Mach numbers. Figure 6 shows the pressure distribution for seven different Mach numbers and the comparison between jet-off and jet-on conditions for $M = 0.90$ to $M = 1.07$. The decrease in positive pressure over the front end of the model with the jet on indicates a reduction in pressure drag.

Pressure drag.- The difference in drag can be more readily seen if $\Delta p/q$ is plotted against the frontal area ratio r^2/R^2. Sample curves

are shown in figure 7 which include jet-on and jet-off conditions for $M = 1.07$ and $M = 1.05$. The area enclosed by such a curve is, with proper regard to sign, equal to the pressure-drag coefficient C_D of the body in presence of the sting, based on frontal area.

Inasmuch as the difference of pressure drag for the two conditions, jet on and jet off, were of primary importance, these values are tabulated in table I. Also taken into consideration is the negative thrust of the jet of air expressed in coefficient form as C_T based on maximum body frontal area. In determining C_T, the rate of air flow in the jet was calculated from the rate of pressure change in the reservoir assuming an adiabatic expansion. The further assumption that the jet exited at $M = 1.0$ fixed the pressure and velocity for the known area of the exit. The formula used in the evaluation was:

$$C_T = \frac{\left[\left(\frac{a_{ex}}{a_1{}^2}\right)\left(\frac{dp}{dt}\right)(V)(\gamma + 1)\right] - \left[p_0 A_{j_{ex}}{}^{\gamma}\right]}{qA_{max}{}^{\gamma}}$$

The amount of reduction in pressure drag varied with Mach number, and the most favorable results were obtained when the jet thrust and Mach number were maximum. Whether the favorable effect was due to a high jet thrust or the high Mach number could not be determined. Data were obtained only for the condition where jet thrust decreased with decreasing Mach number.

Table I shows that, for all conditions tested, a reduction in pressure drag was measured. This reduction in drag $C_{D_j} - C_D$ varied from -0.072 at a Mach number of 1.07 and C_T of -0.047 to -0.023 at a Mach number of 0.90 and a C_T of -0.026. Because of the uncertainty of the actual pressure distribution from the nose $\left(\frac{x}{L} = 0\right)$ to the first orifice $\left(\frac{x}{L} = 0.013\right)$ of the model when the jet was on, the pressure coefficient over this part of the body was considered equal to that of the first orifice. If additional pressure measurements were recorded across this distance, it is believed they would be considerably more negative than assumed in this evaluation. Therefore, the drag reduction for all Mach numbers tested and listed in table I was considered to be conservative in this respect.

Also evaluated was the reduction of drag of the front and rear end of the body separately. This evaluation was obtained by integrating the area between the x-axis and the portions of the curve representing the front and rear ends, respectively. These values are also listed in table I. Because of the relatively small sting size and the rapid curvature of the body at the body-sting juncture, some uncertainty may exist in the rear-end measurements. Nevertheless, the effect upon the rear portion of the body-sting combination at the higher jet thrusts and Mach numbers also indicated a favorable effect.

Shadowgraphs.- In order to understand better the phenomenon of reducing the drag of a body by projecting a jet of air out the front end, a small supersonic tunnel was used to obtain shadowgraphs of the flow conditions. Figure 8 consists of several shadowgraphs taken of the model at a constant Mach number of 1.5 and with the thrust coefficient of the jet varying from 0 to -0.0287. An additional picture, taken in still air with maximum thrust issuing from the jet, is presented in figure 9. It should be noted that the imperfections shown on the pictures are due to the glass of the shadowgraph equipment. The shadowgraphs, obtained at $M = 1.5$, are considered to represent, qualitatively at least, the type of flow that existed at the lower Mach number of the pressure measurements.

As the thrust of the jet is increased, the bow wave is unsteady until a thrust coefficient of -0.0037 is reached. This unsteadiness is observable in figures 8(c) and 8(d) as the result of a multiple-spark photograph. With further increases in thrust, the original bow wave moves forward and a secondary shock wave which first became visible at a thrust coefficient of -0.0016 now travels rearward.

Interpretation of results.- This investigation indicates that the normally high positive pressures at the nose of the body are decreased by the jet; thus the pressure drag was reduced. A study of the shadowgraphs and the pressure distributions has led to the concept that the jet in acting on the surrounding flow produces a strong vortex ring near the nose of the body. The high negative pressures measured in the neighborhood of the nose according to this concept indicate that a forward flow of high velocity is induced in this region. Further consideration of this proposed flow leads to the possibility of the existence of a stagnation ring behind the body nose. The examination of the pressure distributions of figure 6 shows that, should such a stagnation ring exist, it must lie at approximately $\frac{x}{L} = 0.03$. There was no evidence in the recorded data to indicate that a stagnation ring at any time lay at one of the orifice positions, although it is not reasonable to expect the stagnation ring to remain fixed for all jet exit

conditions. The effect of a small angle of attack combined with the method of averaging the pressure between upper and lower orifices would tend to prevent the recording of full stagnation pressure on the side of the body. Presuming a side stagnation point is present on the body and the pressure-drag reduction is revaluated, the pressure drag in terms of drag coefficient will then be increased about 0.045. This increase in drag coefficient is considered maximum and the actual value could be anywhere from 0.045 to 0.

If a jet is exhausted rearward, the entire thrust is utilized in propulsion. If, however, the jet is expelled forward, the thrust of the jet is negative and opposes the motion of the body. A so-called thrust recovery factor may be defined by

$$TRF = \frac{\left(C_{D_j} - C_D\right) - C_T}{C_T}$$

This thrust recovery factor is simply the excess of drag reduction over the rearward thrust produced by the forward jet divided by the thrust to be expected from a rearward jet. The drag reduction was determined from the changes in pressure drag only; no estimate of the changes in viscous drag have been included. It is pointed out that, properly, the thrust of the rearward jet should be measured on an actual body without a sting so as to take into account the interaction between the external flow and the rearward jet. Note that, for the forward jet to produce a net force on the body equivalent to that expected of a rearward jet, the drag reduction of the body would have to be twice the thrust of the jet. In the measurements reported herein, the thrust recovery factor was at best only 0.532. Perhaps investigation of a configuration specifically designed for this purpose would result in an increase in the thrust recovery factor.

CONCLUDING REMARKS

From preliminary studies of pressure-drag reduction obtained by projecting a jet of air from the nose of a prolate spheroid, the following characteristics appear significant:

(a) The energy in the jet relative to the free stream

(b) The mixing process in the free jet or the jet Reynolds number

(c) The slope of the body and the jet size relative to the body size

The available evidence indicates that, at low jet energies, the pressure-drag reduction all but disappears. Measurements made at a high jet thrust and zero forward speed showed a negligible effect of the jet on the pressures of the body.

The higher the shear at the jet exit, the lower is the pressure that can be induced by the jet. In this respect, a heated jet would undoubtedly give rise to a difference in the pressure-drag phenomena.

It seems likely that, since the minimum pressure occurs at the jet exit, the slope of the body at that point should be maximum for the maximum favorable effect.

The preliminary tests reported do not show promise that this scheme is useful for propulsion, but it would indeed be a rare coincidence if all the important factors were optimum. It seems more to the point to note that a jet directed forward from the nose of the body did alter the pressure distribution in such a way that the pressure drag of the body was reduced. Thus, in a restricted sense, the nose jet produced a thrust on the body.

Langley Aeronautical Laboratory
National Advisory Committee for Aeronautics
Langley Field, Va.

REFERENCES

1. Johnston, J. Ford, and Lopatoff, Mitchell: Study by NACA Wing-Flow Method of Transonic Drag Characteristics of a Blunt-Nose Body of Revolution and Comparison with Results for a Sharp-Nose Body. NACA RM L9C11, 1949.

2. Huguenard, E.: High Velocity Wind Tunnels. (Their Application to Ballistics, Aerodynamics and Aeronautics.) NACA TM 318, 1925.

3. Hebrank, W. H., and Hicks, B. L.: A Preliminary Study of the External Ram Jet. Rep. No. 522, Ballistic Res. Lab., Aberdeen Proving Ground, Oct. 1950.

4. Yeates, John E., Jr., Bailey, F. J., Jr., and Voglewede, T. J.: Apparatus for Obtaining a Supersonic Flow of Very Short Duration and Some Drag Measurements Obtained with Its Use. NACA RM L9C01, 1951.

TABLE I

OBSERVED VALUES OF DRAG COEFFICIENT

AND THRUST RECOVERY FACTOR

M	C_T	C_D Total	$C_{D_j} - C_D$ Total	$C_{D_j} - C_D$ Nose	$C_{D_j} - C_D$ Tail	TRF
0.90	-0.026	0.010	-0.023	-0.026	0.003	-0.115
.95	-.032	.010	-.024	-.033	.009	-.250
1.02	-.036	.165	-.031	-.032	.001	-.139
1.03	-.038	.173	-.032	-.021	-.011	-.158
1.04	-.037	.192	-.039	-.022	-.017	.054
1.05	-.043	.198	-.064	-.038	-.026	.488
1.07	-.047	.211	-.072	-.049	-.023	.532

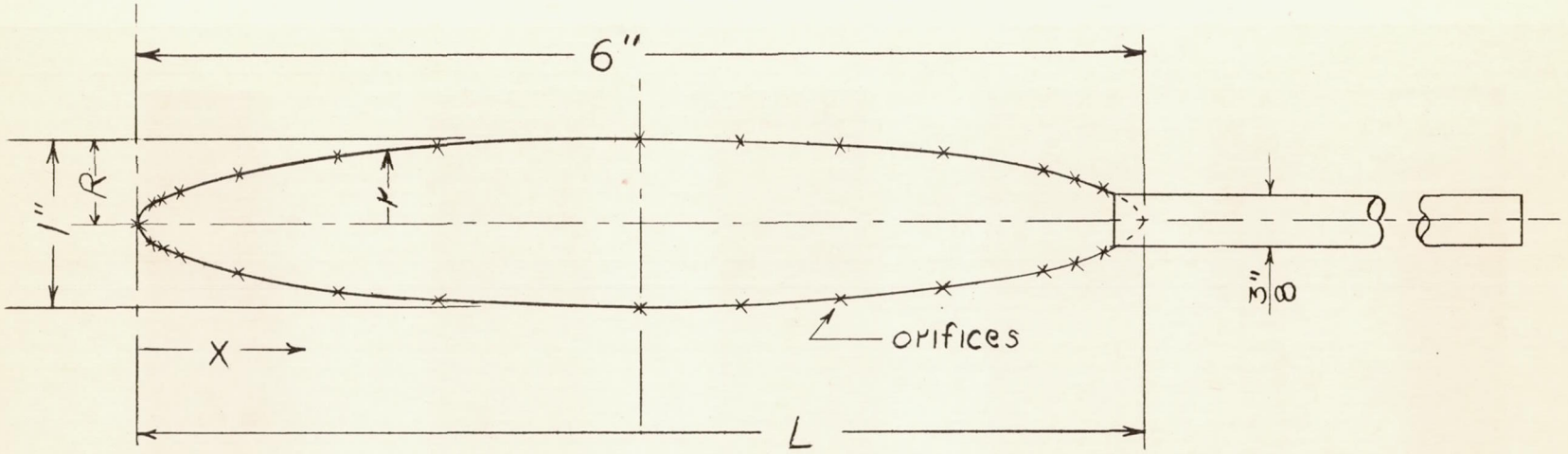

TABLE OF ORDINATES

x Inches	r Inches	x Inches	r Inches
0	0	2.600	0.495
.050	.091	3.000	.500
.090	.121	3.400	.495
.200	.179	3.800	.482
.600	.300	4.200	.458
1.000	.373	4.600	.423
1.400	.423	5.000	.373
1.800	.458	5.400	.300
2.200	.482	5.785	.182

ORIFICE LOCATIONS

x/L	
0	0.500
.013	.600
.023	.700
.043	.800
.100	.900
.200	.933
.300	.959

Figure 1.- Sketch of the prolate spheroid body showing dimensions and orifice locations.

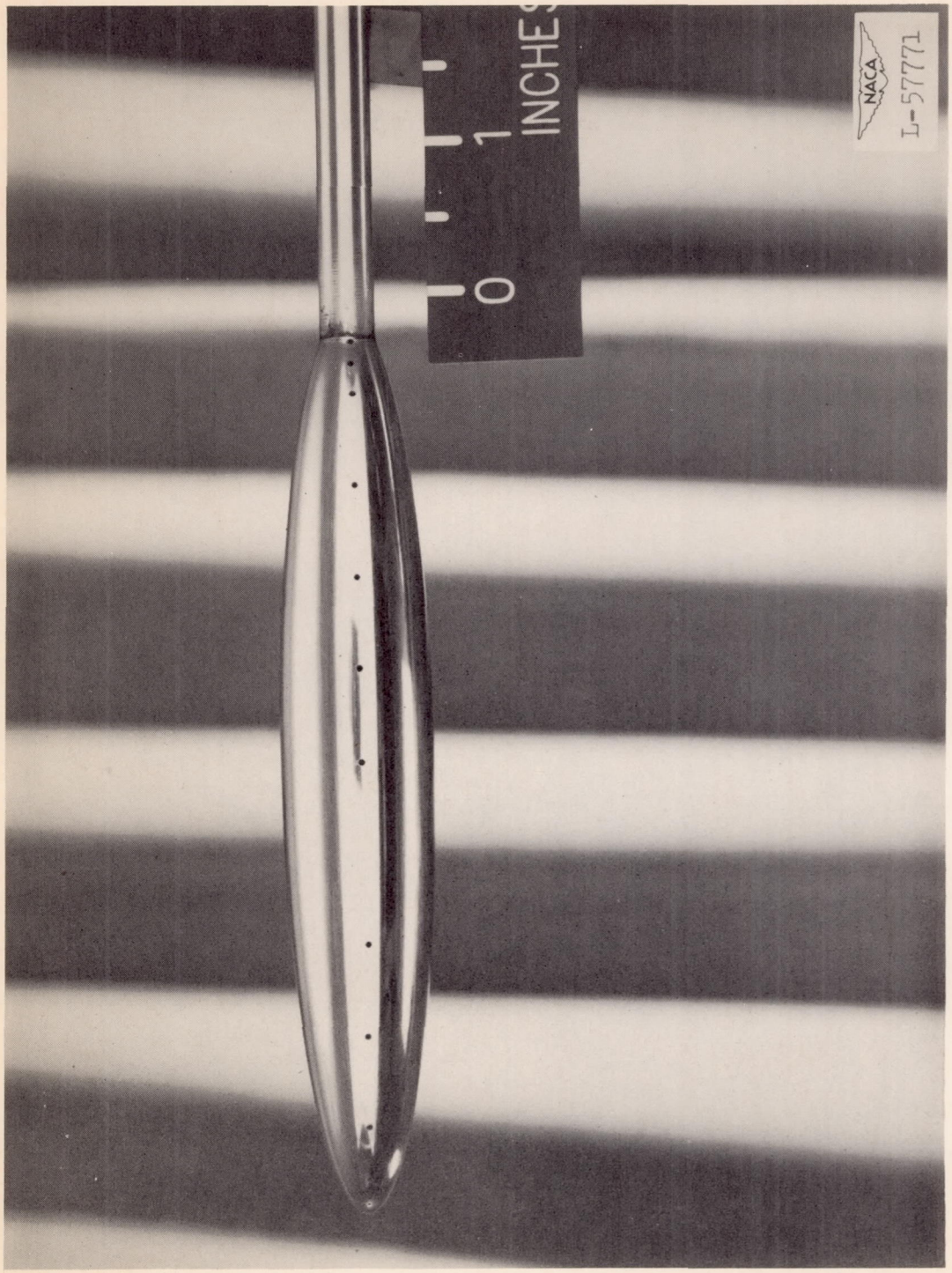

Figure 2.- Prolate spheroid body.

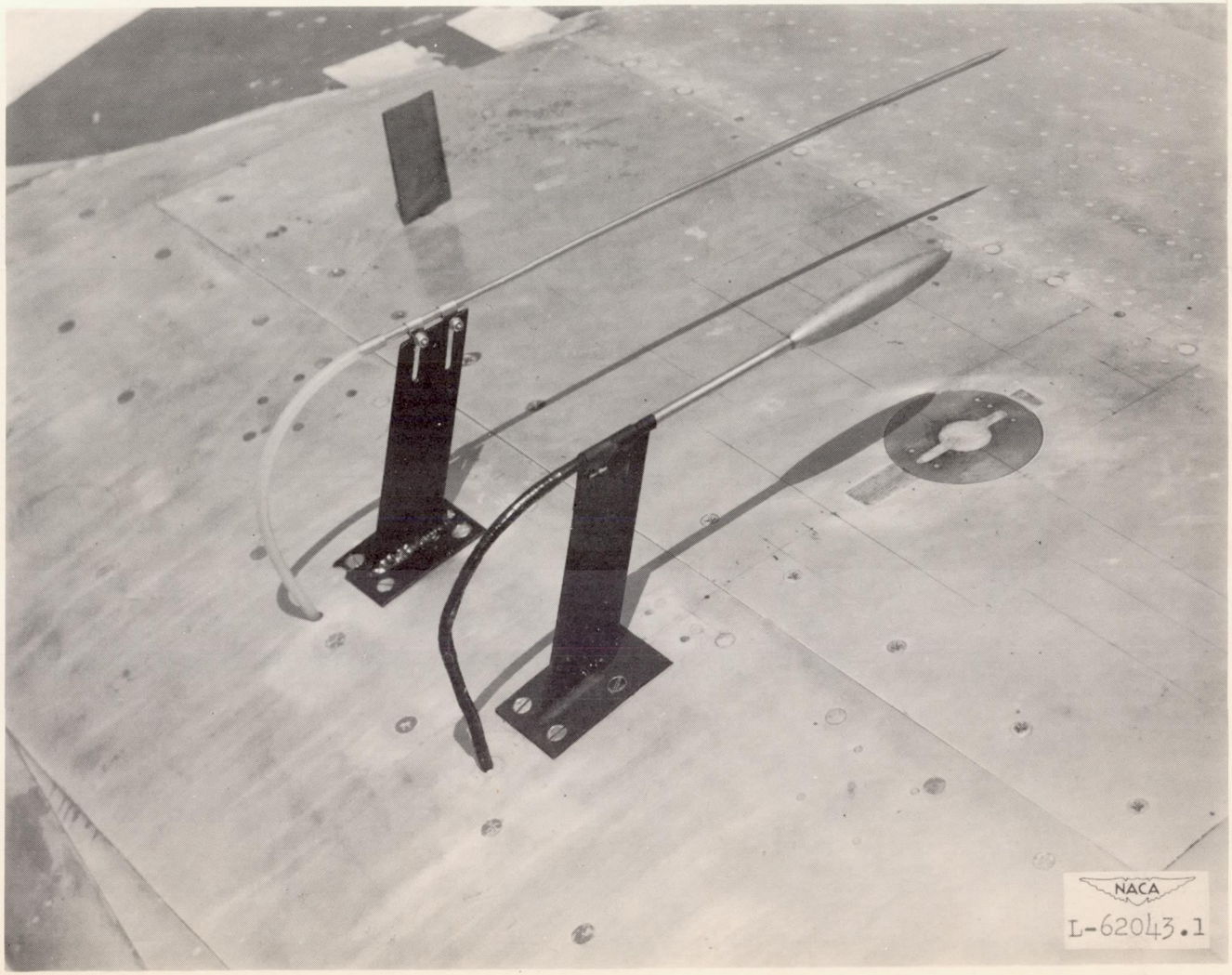

Figure 3.- Body-sting combination mounted on airplane wing with reference static-pressure tube.

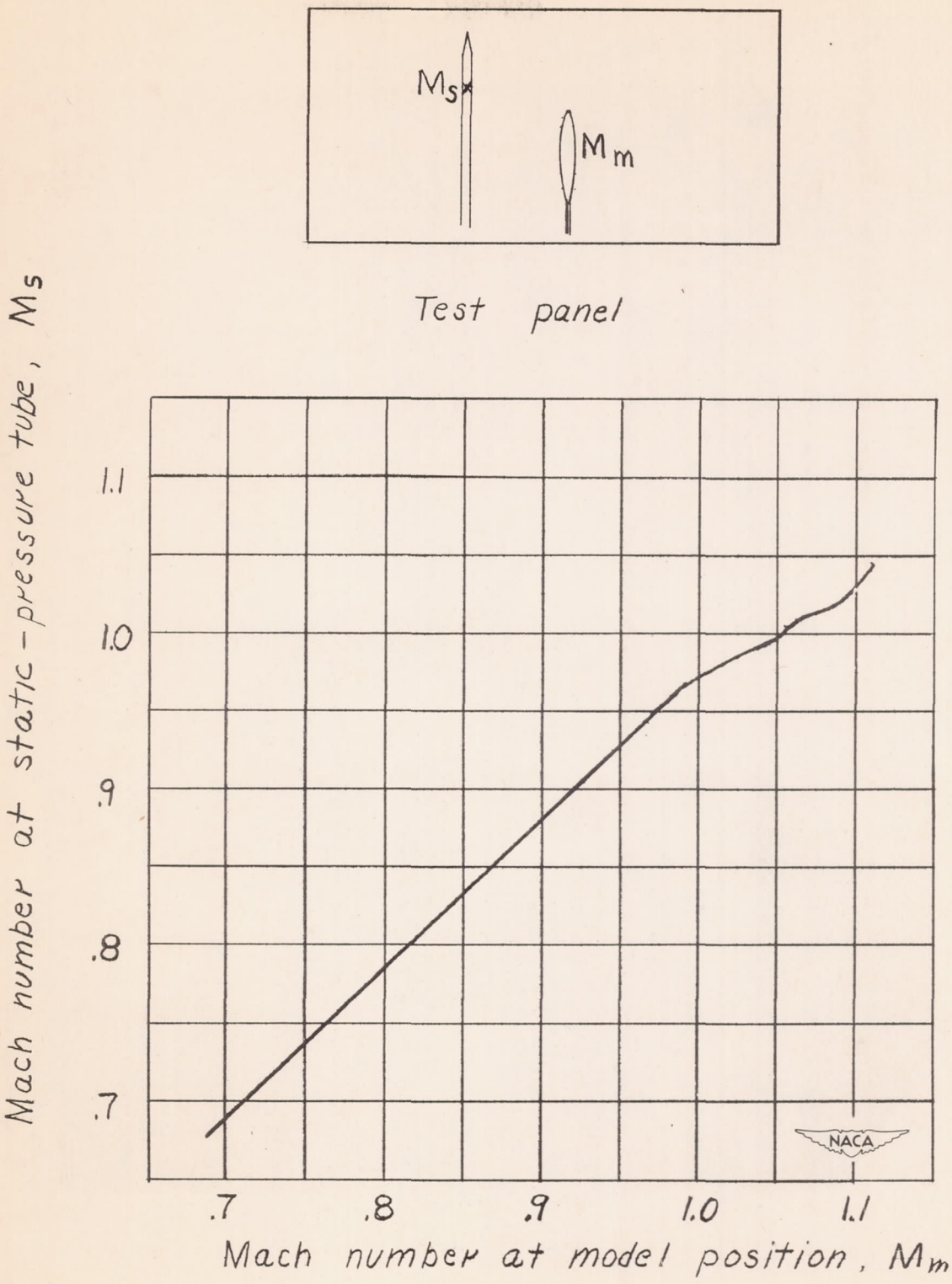

Figure 4.- Calibration of test panel.

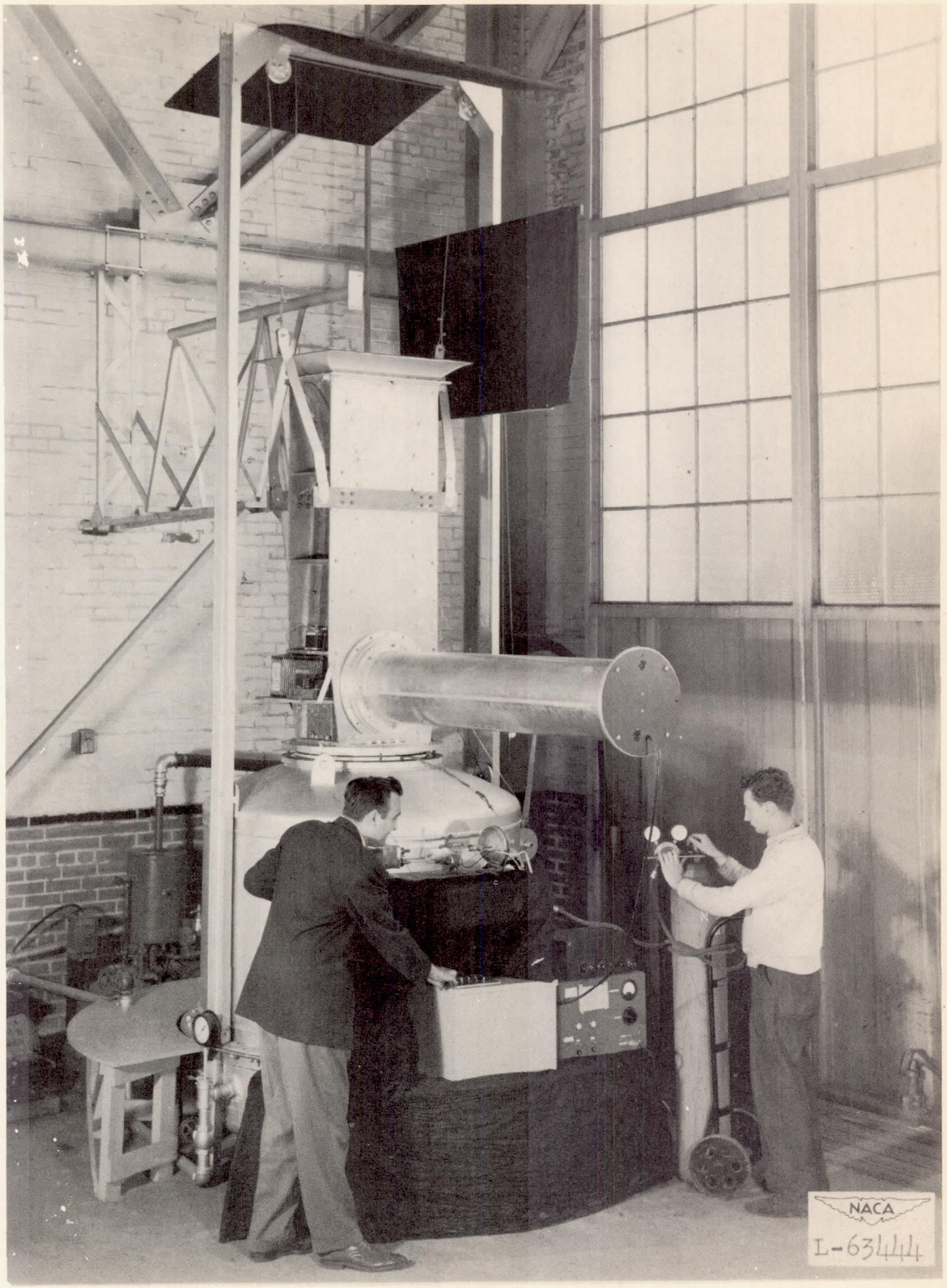

Figure 5.- Supersonic tunnel with shadowgraph equipment.

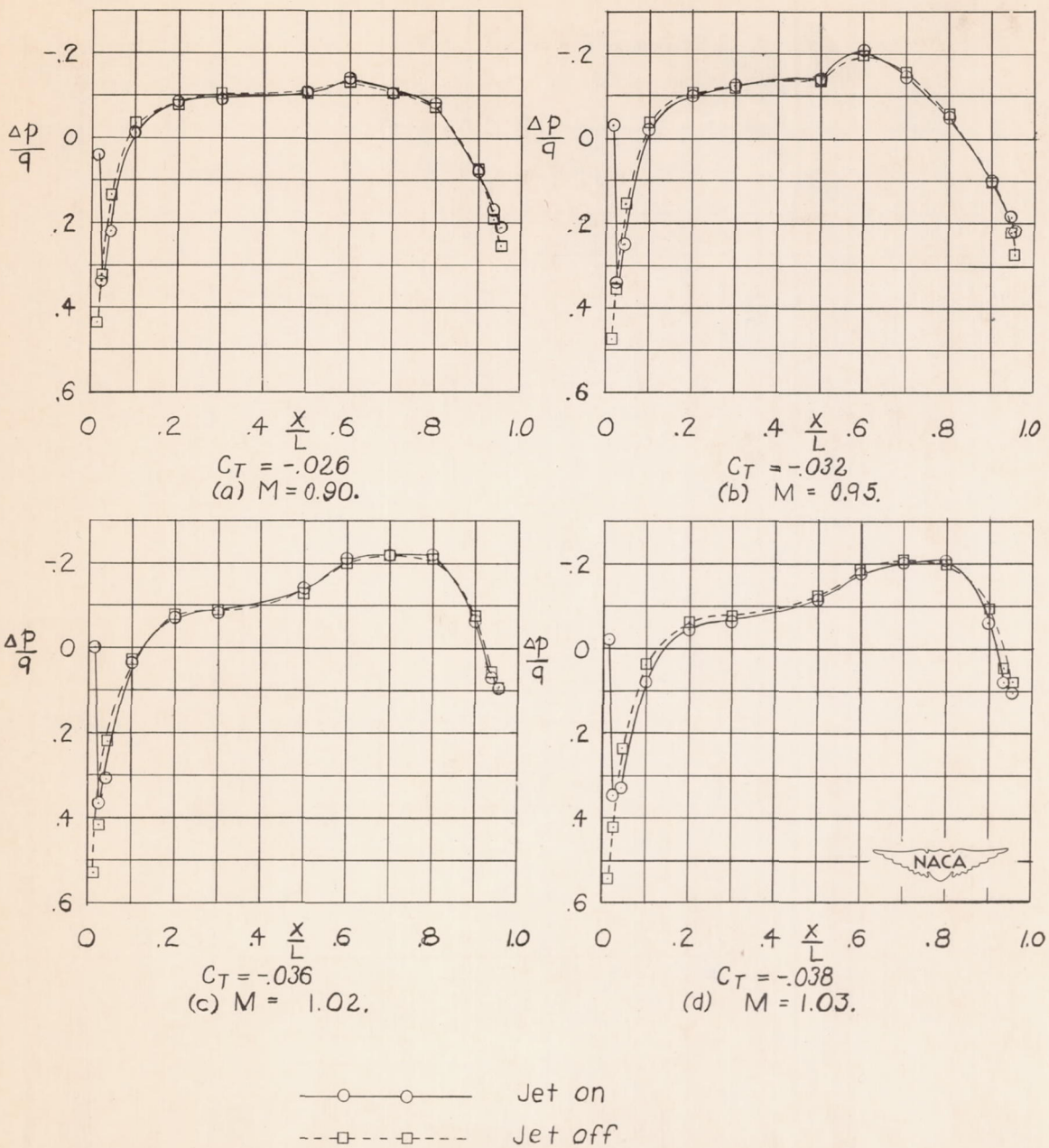

Figure 6.- Pressure distribution along axis for various Mach numbers.

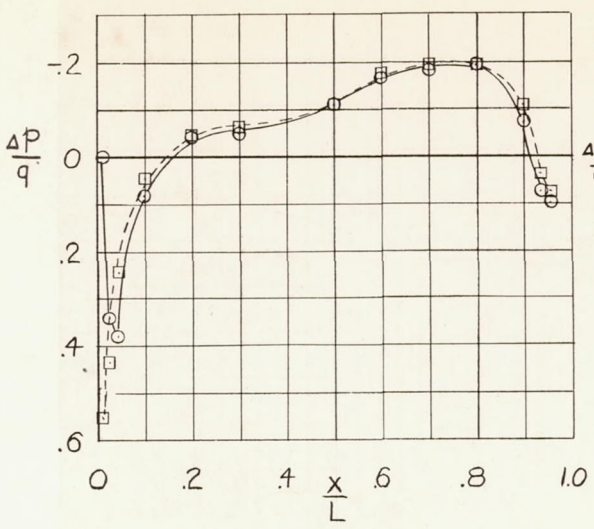

$C_T = -.037$

(e) M = 1.04.

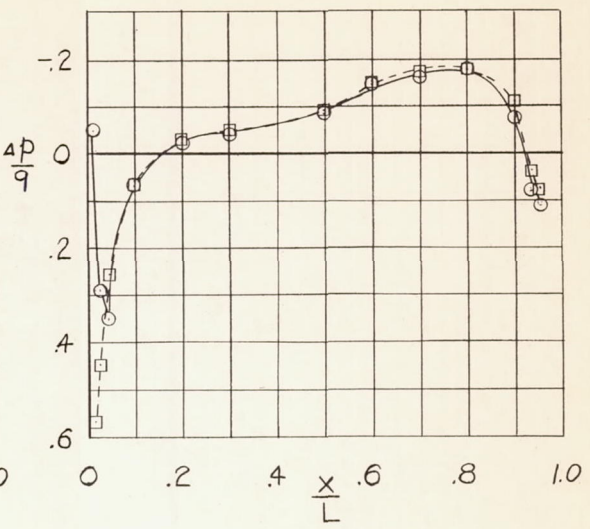

$C_T = -.043$

(f) M = 1.05.

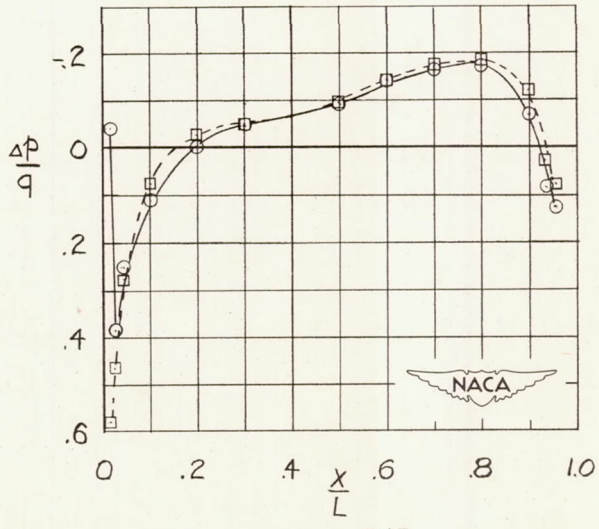

$C_T = -.047$

(g) M = 1.07.

Figure 6.- Concluded.

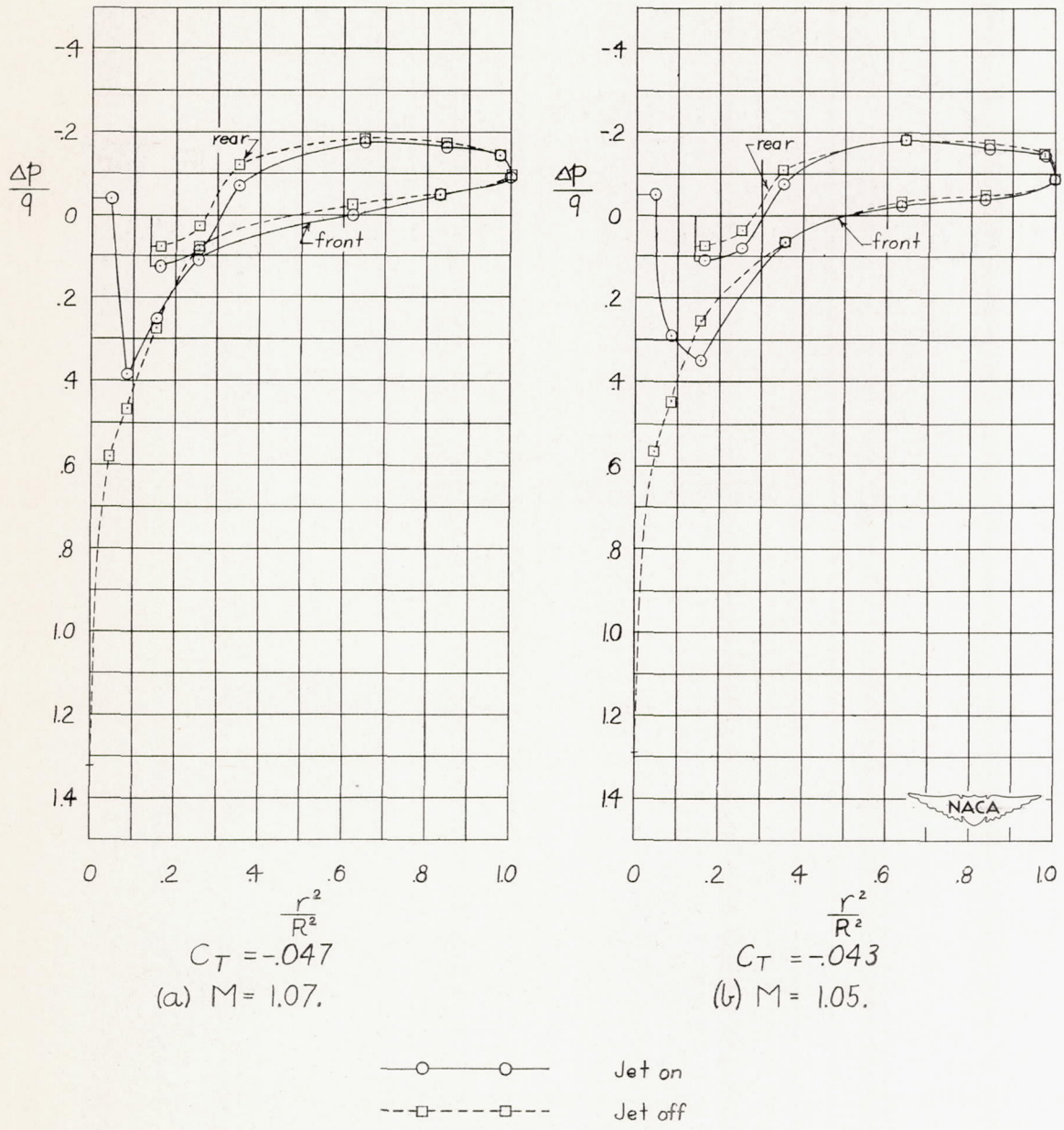

$C_T = -.047$

(a) M = 1.07.

$C_T = -.043$

(b) M = 1.05.

Figure 7.- Sample plots of $\Delta p/q$ against $(r/R)^2$ used in determining the value of the pressure-drag coefficient.

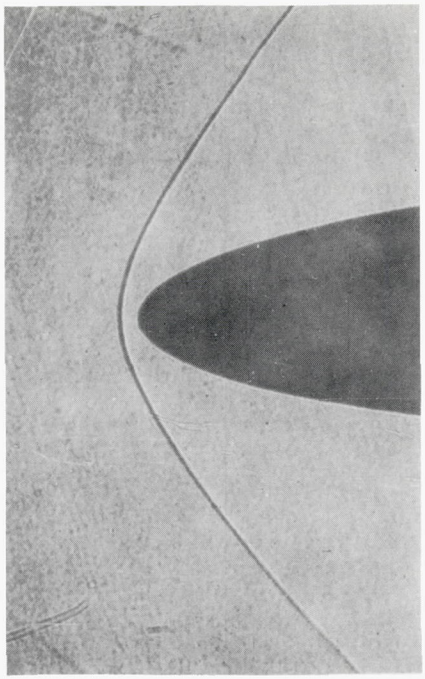

(a) $C_T = 0.$

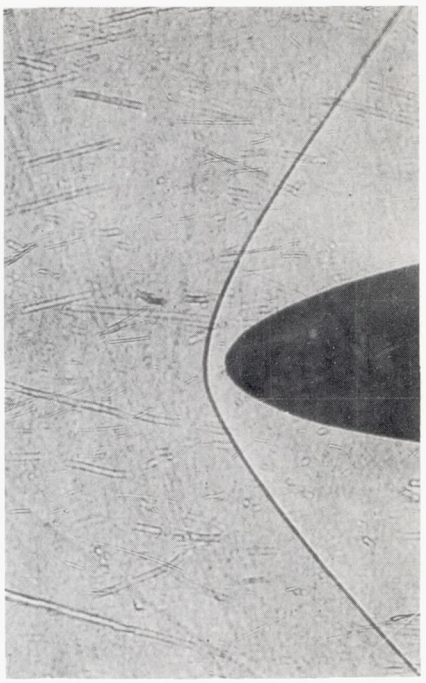

(b) $C_T = -0.0003.$

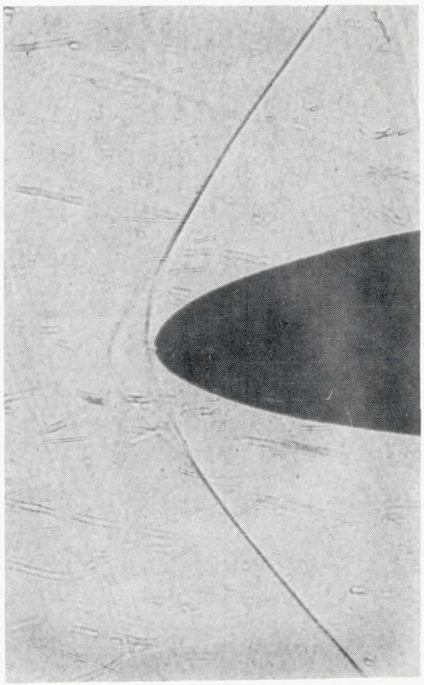

(c) $C_T = -0.0016.$

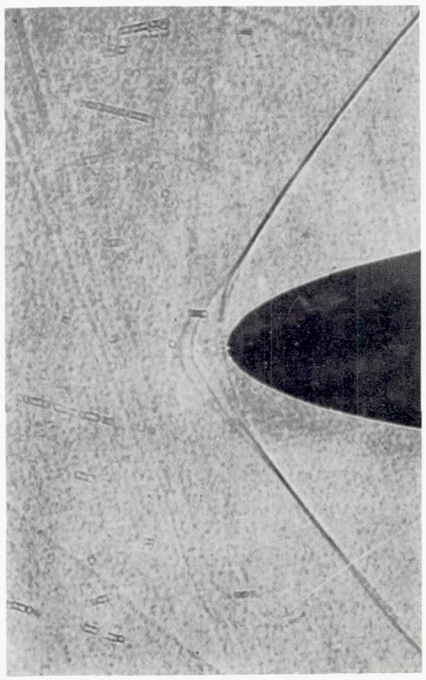

(d) $C_T = -0.0037.$

NACA L-69140

Figure 8.- Shadowgraphs of model at M = 1.5.

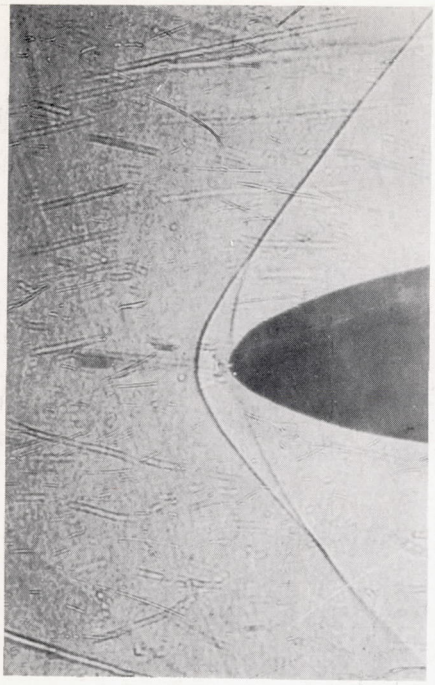

(e) $C_T = -0.0088$.

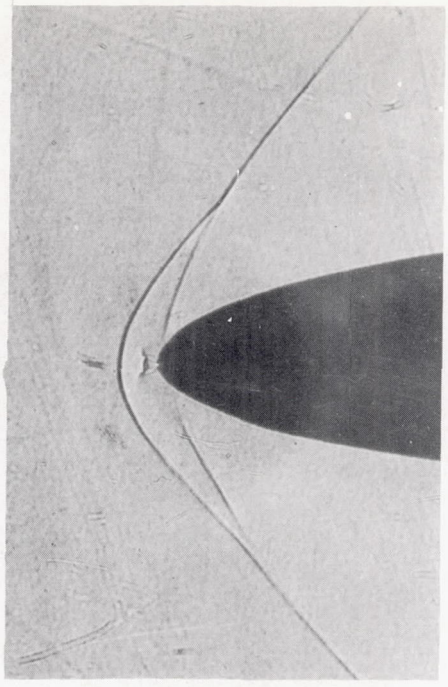

(f) $C_T = -0.0149$.

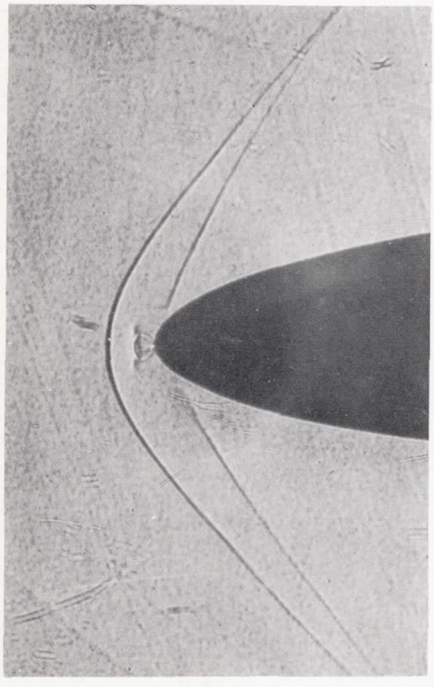

(g) $C_T = -0.0216$.

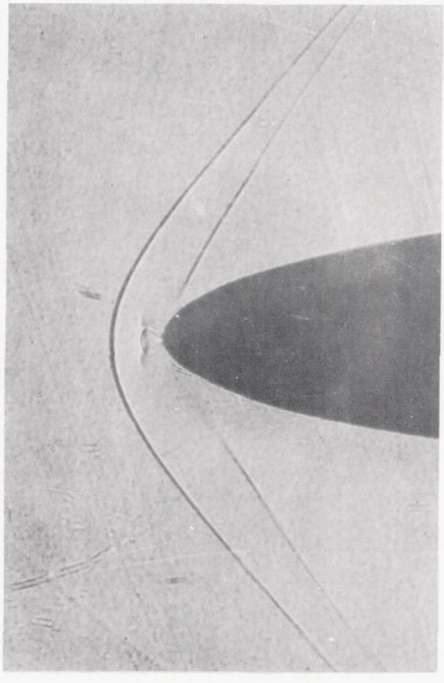

(h) $C_T = -0.0287$.

NACA L-69141

Figure 8.- Concluded.

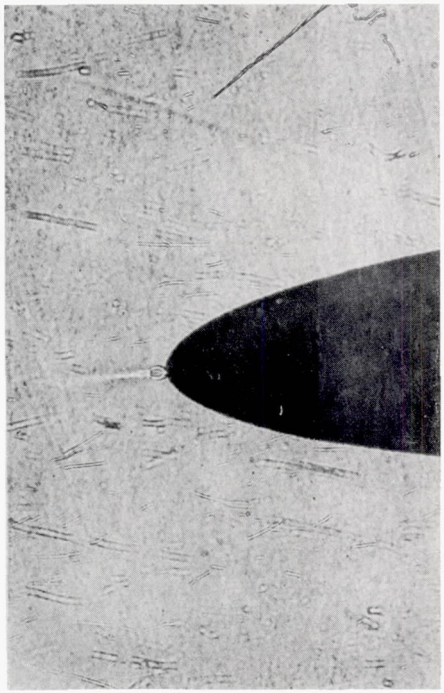

L-69142

Figure 9.- Shadowgraph of model in still air. C_T = -0.0287 (based on dynamic pressure at M = 1.5).